# COMPUTER SIMULATION OF STRUCTURE OF MOLTEN $DyF_3$-$BaF_2$-LiF SYSTEM BY MONTE CARLO METHOD①

Xu Chi, Su Hang, Chen Nianyi
*Shanghai Institute of Metallurgy, Chinese Academy of Sciences, Shanghai 200050*

**ABSTRACT** The structure of molten $DyF_3$-$BaF_2$-LiF system has been computer-simulated by Monte Carlo method. The radial distribution functions (RDFs), the local structure as well as the energy distribution have been obtained. The study indicates that $F^-$ ions distribute closely around $Dy^{3+}$ ions and mainly form octahedral complex ions like $DyF_6^{3-}$. There exist some "free" $Li^+$ ions in the molten system, which have the highest potential energy and are current-carrying ions in the electrolytic process. $F^-$ ions may be classified into three types: "terminal fluoride", "free fluoride" and "bridge fluoride", which have different behaviours and potential energies. Some complex ions like $DyF_m^{3-m}$ clusters are connected to one another by "fluoride-bridge", forming more complicated ionic clusters like $F_m$-Dy-F-Dy-$F_n$ or $F_m$-Dy $<^{F}_{F}>$ Dy-$F_n$. As compared with molten $DyF_3$-LiF system, the octahedral complex ions like $DyF_6^{3-}$ seem closer and in better order than the binary system because of the addition of $BaF_2$.

**Key words** rare-earth fluoride molten salt computer simulation Monte Carlo method local structure

## 1 INTRODUCTION

The rare-earth fluoride melts with high melting points are corrosive, hence the direct experimental determination of their structure and physicochemical characters is rather difficult. Therefore it is short of methods of studying local structures of the melts on atomic level. In recent years, the thermodynamic characters of many alkaline metal halide melts have been successfully calculated by computer simulation methods, such as Monte Carlo method and Molecular Dynamics method[1]. Using these methods, the structures of some molten solutions[2-5] have been investigated, and some thermodynamic properties, including the RDFs and local structures of the rare-earth chloride and fluoride molten salts[6-7] which are rather difficult to be directly determined, have been calculated. The simulation results of $DyF_3$-LiF-$BaF_2$ (molar ratio 3∶6∶1) molten system by using Monte Carlo method are reported in this paper.

## 2 MODEL AND METHOD

By the usually used Metroplis procedure[8] and periodic boundary condition with a unit cell containing some ions, a computer program of Monte Carlo method for liquid structure simulation was used in computation. The principle has been explained in reference[2].

In this work, the cubic unit cell contains 216 ions, including 24 $Dy^{3+}$ ions, 48 $Li^+$ ions, 8 $Ba^{2+}$ ions and 136 $F^-$ ions, which is equal to 24 $DyF_3$"molecules", 48 LiF "molecules" and 8 $BaF_2$"molecules", or corresponds to $DyF_3$-LiF-$BaF_2$ system with molar ratio $DyF_3$ ◇LiF ◇$BaF_2$ = 3 ◇6 ◇1. The temperature of the simulated system is 1073 K.

Born[9] potential function is used to describe the interaction potential energy among $Dy^{3+}$, $Ba^{2+}$, $Li^+$ and $F^-$ ions:

① Received Jan. 8, 1996; accepted Apr. 18, 1996

$$E_{ij} = \frac{Z_i Z_j}{r_{ij}} + \frac{b}{r_{ij}^n}$$

$$b = - Z_i Z_j (R_i + R_j)^{n-1} / n$$

where $E_{ij}$ is the potential energy of $i$ ion with $j$ ion; $r_{ij}$ is the distance between the ions; $Z_i$, $Z_j$ are the valence numbers; $R_i$, $R_j$ are the ionic Goldschmidt radii of ion $i$ and $j$ respectively. The value of $n$ is 7 in this case. In order to avoid the mutual penetration between ions, it has been assumed that $E_{ij} = \infty$ when $r_{ij} < 0.7 (R_i + R_j)$.

The simulated system approaches Boltzmann distribution and total energy approaches equilibrium value after more than $10^5$ steps of computation. The computational results can be used as source information about the structure of the melt. The instantaneous coordinates of ions and other structure parameters can be obtained from these results.

## 3 RESULTS

### 3.1 Instantaneous structure

Fig. 1 illustrates an example of the instantaneous arrangement of ions in $DyF_3$-$BaF_2$-LiF molten system at 1 073 K. It can be seen from Fig. 1 and the section figure of the instantaneous structure that the gaps and holes between ions are not uniformly distributed in $DyF_3$-$BaF_2$-LiF molten system. $Dy^{3+}$ ions are surrounded by a large number of $F^-$ ions. Some $F^-$ ions overlap partly. Some complex ions in form of $DyF_n^{3-n}$ clusters are connected to each other by fluoride-bridge ($F_m$-Dy $<^{F}_{F}>$ Dy-$F_n$ or $F_m$-Dy-F-Dy-$F_n$), forming more complicated clusters like $Dy_mF_n^{3m-n}$. On the contrary, $Li^+$ ions exist in free state, not forming complex ions like $Li_mF_n^{m-n}$ clusters.

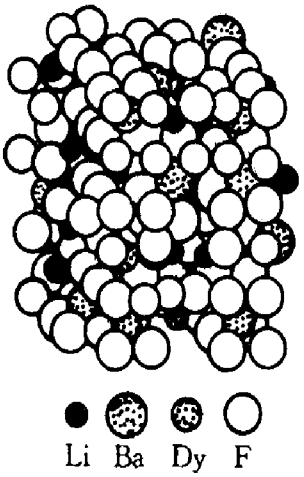


**Fig. 1 An example of instantaneous ionic distribution in $DyF_3$-$BaF_2$-LiF melt at 1 073 K**

### 3.2 Radial distribution functions

The radial distribution functions(RDFs) of $Dy^{3+}$-$F^-$ ion pair are illustrated in Fig. 2. The main peak in the partial RDF of $Dy^{3+}$-$F^-$ ion pair locates at $r$ = 0.225 nm, which is lower than the sum of the two ionic radii ($Dy^{3+}$ : 0.107 nm; $F^-$ : 0.133 nm). The tail of the main peak locates at $r$ = 0.315 nm, which can be regarded as the first coordination radius of $Dy^{3+}$ ion surrounded by $F^-$. Within this distance, the percentage of $Dy^{3+}$ ions with six $F^-$ neighbours is about 83.3% and that with five $F^-$ neighbours is about 16.7%. The average number of $F^-$ ions around $Dy^{3+}$ ions is 5.83. So a large number of $Dy^{3+}$ ions form octahedral complex-ions like $DyF_6^{3-}$ clusters. In addition, there exist a few $DyF_5^{2-}$ clusters and some complicated complex ionic clusters linked by fluoride-bridge.

The main peak in the curve of partial RDF of $Li^+$-$F^-$ pair locates at $r$ = 0.255 nm (Fig. 3),

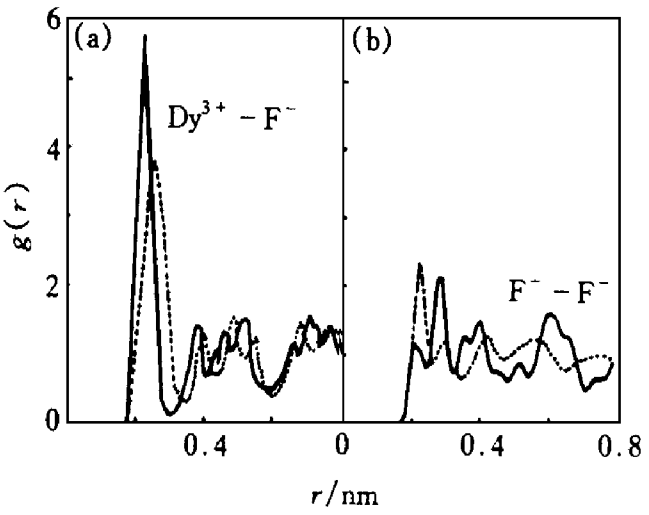


**Fig. 2 Partial RDFs of $Dy^{3+}$-$F^-$ (a) and $F^-$-$F^-$ (b) ion pairs**

solid line—in $DyF_3$-$BaF_2$-LiF melt;
dotted line—in $DyF_3$-LiF melt

which is far more than the sum of radii of the two ions ($Li^+$: 0.078 nm). Moreover, the least distance between the two ions is $r$ = 0.215 nm, which is also more than the sum of radii of the two ions. Such a phenomenon arises rarely in contrary ionic partial RDFs.

The RDF of $Ba^{2+}$-$F^-$ ion pair is also illustrated in Fig. 3. The main peak in the curve of partial RDF of $Ba^{2+}$-$F^-$ ion pair locates at $r$ = 0.265 nm. The tail of main peak locates at $r$ = 0.355 nm. The height of the main peak is 4.62. Within the first coordination radius (0.355 nm) of $Ba^{2+}$ surrounded by $F^-$ ions, the percentage of $Ba^{2+}$ ions with five $F^-$ neighbours is about 50% and that with four $F^-$ neighbours is about 50%. The average number of $F^-$ ions around $Ba^{2+}$ ions is 4.5.

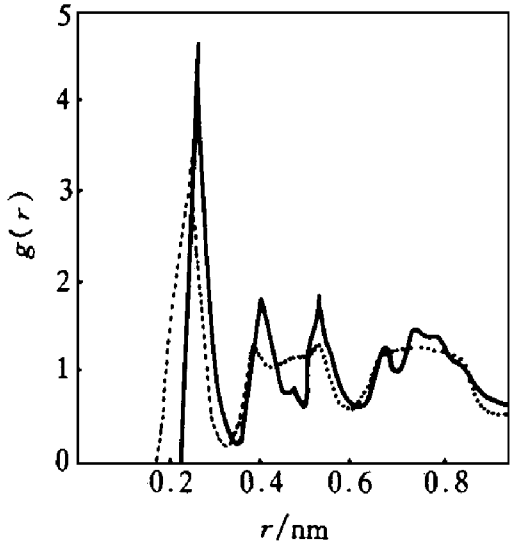


**Fig. 3 Partial RDFs of $Ba^{2+}$-$F^-$ and $Li^+$-$F^-$ ion pairs in $DyF_3$-$BaF_2$-LiF melts**

solid line—$Ba^{2+}$-$F^-$; dotted line—$Li^+$-$F^-$

The main peak in the curve of partial RDF of $F^-$-$F^-$ ion pair locates at $r$ = 0.285 nm (see Fig. 2), which is more than the sum of the two ionic radii. There exists a secondary peak before the main peak. Generally speaking, the location of the main peak in the curve of partial RDF of the same kind of ions is bound to exceed the sum of the two ionic radii. But the position of the secondary peak in this case locates at $r$ = 0.255 nm, which is lower than the sum of the two ionic radii. The reason is that there are a large number of $F^-$ ions around $Dy^{3+}$ ions, and since the radius of $F^-$ ion exceeds that of $Dy^{3+}$ ion, some $F^-$ ions overlap partly. But most of $F^-$ ions do not overlap on each other, which can be illustrated from the location of the main peak.

### 3.3 Potential energy distribution

The potential energy distribution was analyzed by calculating the potential energies of $Dy^{3+}$, $Ba^{2+}$, $Li^+$ and $F^-$ ions. The average potential energies of the following ions are: $Dy^{3+}$ $-11.4\times10^{-18}$ J, $Li^+$ $-2.22\times10^{-18}$ J, $Ba^{2+}$ $-5.20\times10^{-18}$ J and $F^-$ $-2.09\times10^{-18}$ J, respectively. The average potential energy of $Li^+$ ions is obviously higher than those of $Dy^{3+}$ and $Ba^{2+}$ ions, which shows that $Li^+$ ions are active ones, acting as current-carrying ions in electrolytic process. Fig. 4 illustrates the potential energy distribution of $F^-$ ions. The main peak of the curve locates at $-2.05\times10^{-18}$ J, but the tail of the peak extends as far as $-3.45\times10^{-18}$ J, i.e. the energies of a few $F^-$ ions are lower, which may be related to their different micro-environment. Some $F^-$ ions distribute closely around two $Dy^{3+}$ ions with higher charge, so their potential energies are certainly lower.

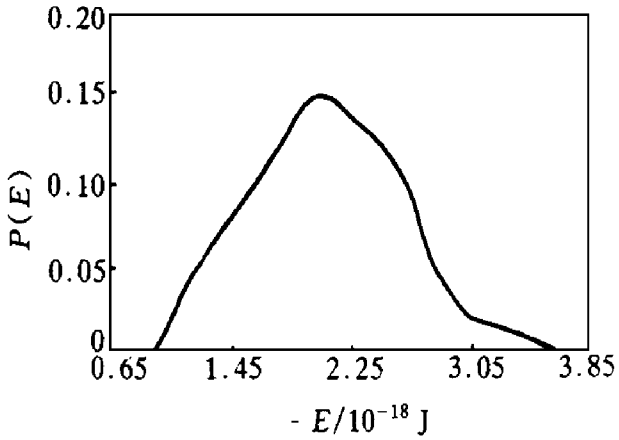


**Fig. 4 Potential energy distribution of $F^-$ ions in $DyF_3$-$BaF_2$-LiF melt**

### 3.4 Bond angle distribution

Within the first coordination radius around $Dy^{3+}$ ion, the peak values of bond angle distribution of $\angle F^-$-$Dy^{3+}$-$F^-$ locating at 71° and 113° are almost the same, see Fig. 5. As indicated above, the form of $Dy^{3+}$ ion with six $F^-$ neighbours is far more than others, so details of the

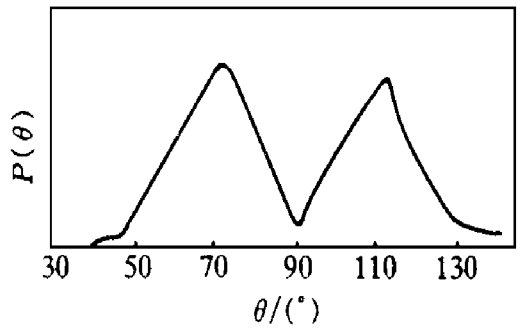


**Fig. 5 Bond angle distribution of $\angle F^- - Dy^{3+} - F^-$ in $DyF_3$-$BaF_2$-LiF melt**

octahedral structure of $DyF_6^{3-}$ type ions can be determined.

## 4 DISCUSSION

### 4.1 Effect of $BaF_2$

We have reported the computer simulation results about $DyF_3$-LiF (molar ratio 3: 7) melt system earlier[7]. In this paper, keeping the mole fraction of $DyF_3$ (30%) constant, LiF was partially replaced with 10% (in mole) $BaF_2$. Compared with the results of reference[7], the effect of $BaF_2$ can be seen as follows:

(1) The octahedral complex ions of $DyF_6^{3-}$ type become closer. See Fig. 2, the location of main peak in the partial RDF of $Dy^{3+}$-$F^-$ pair decreases from 0.255 to 0.225 nm, and the radius of the first coordination sphere decreases from 0.355 to 0.315 nm, while the height of main peak increase from 3.78 to 6.43.

(2) Although the average distance between $Dy^{3+}$ and surrounding $F^-$ decreases, the overlap between $F^-$ and $F^-$ decreases instead of increases. From Fig. 2 it can be seen that, the location of main peak in the partial RDF of $F^-$-$F^-$ ion pair increases from 0.215 (less than their radial sum) to 0.285 nm, but a secondary peak ($r$ = 0.255 nm, less than the radial sum of two $F^-$ ions) in front of the main peak shows the overlap between some $F^-$ ions around $Dy^{3+}$.

In general, as a result of the addition of $BaF_2$, the form of $DyF_6^{3-}$ type octahedral complex ions seems more orderly than that in $DyF_3$-LiF melt system, which may affect some physical properties of the melt (or rapid-colding amorphous glass). The details will be reported later.

### 4.2 Classification of $F^-$ ions around $Dy^{3+}$

According to the simulation result that the tail of the first peak in the partial RDF of $Dy^{3+}$-$F^-$ pair locates at $r$ = 0.315 nm, $F^-$ ions within the first coordination radius of one $Dy^{3+}$ ion are called "terminal fluoride", $F^-$ ions within that of two or more $Dy^{3+}$ ions are called "bridge fluoride", and $F^-$ ions outside that of $Dy^{3+}$ ions are called "free fluoride".

The percentages of "terminal fluoride" and "free fluoride" are 51.5% and 24.2%, respectively. The percentage of "bridge fluoride" is about 24.3%, most of which locate within the first coordination radius of two $Dy^{3+}$ ions, while a few within that of three $Dy^{3+}$ ions. The potential energy of "bridge fluoride" is the lowest, while that of "terminal fluoride" is somewhat higher, and that of "free fluoride" is the highest. It is obvious that in molten state the coordination form of each $F^-$ ion is variable.

## REFERENCES

1 Larsen B, Forland T. Mol Phys, 1973, 26: 1521.
2 Chen Nianyi, Xu Chi, Jiang Naixiong, Li Tonghua. Scientia Sinica, (Series B), 1987, 30: 1029.
3 Xu Chi, Jiang Naixiong, Chen Nianyi. Acta Chim Sinica, (in Chinese), 1989, 47: 529.
4 Xu Chi, Chen Nianyi, Jiang Naixiong. Acta Phys Chem Sinica, (in Chinese), 1987, 3: 55.
5 Xu Chi, Jiang Naixiong, Chen Nianyi. Acta Metallurgica Sinica, (Series B), 1992, 5: 145.
6 Yang Zhongbao, Guo Chuntai, Tang Dingxiang, Xu Chi. J Chinese Rare Earth Society, (in Chinese), 1991, 9: 20.
7 Xu Chi, Liu Ji, Chen Nianyi, Li Jie, Tang Dingxiang. J Rare Earths, 1993, 11: 170.
8 Metropolis N A, Rosenblutu A W *et al*. J Chem Phys, 1953, 21: 1067.
9 Born M, Lande A. Verh Dent Physik Ges, 1918, 20: 210.

**(Edited by Li Jun)**